საქართველოს მეცნიერებათა ეროვნული აკადემიის მოამბე, ტ. 18, №2, 2024
BULLETIN OF THE GEORGIAN NATIONAL ACADEMY OF SCIENCES, vol. 18, no. 2, 2024

Materials Science

Smart Nanocomposite in TiC-BN-SiC-B_4C-SiAlON-Al_2O_3 System for Turbine Disks and Wings, Ballistic Armor for Operation in Hot Nodes of Flying Machines

Zviad Kovziridze[*], Natela Nizharadze[*], Maia Mshvildadze[*], Gulnazi Tabatadze[*], Temur Cheishvili[*], Tsira Danelia[*], Nino Darakhvelidze[*], Maia Balakhashvili[*], Salome Gvazava[*]

[*] *Institute of Bionanoceramics and Nanocomposite Technology, Bionanoceramic and Nanocomposite Science Center, Georgian Technical University, Tbilisi, Georgia*

(Presented by Academy Member Vladimir Tsitsishvili)

Our objective was to obtain β – SiALON-containing nanocomposites at the first stage using reactive sintering method at 1400°C, with nitriding process in the TiC-BN-SiC-B_4C-Si-Al-Al_2O_3 system and study the phase composition of received consolidated materials in the TiC-TiB_2-BN-SiC-B_4C-β-SiAlON-Al_2O_3 (nanopowder-400 nm) system. The obtained composite was ground in an attritor and the consolidated composite was obtained by hot pressing at 1620°C for 40 minutes, with glassy perlite (Armenia) dope 2 mass%, with 8-minute hold at the final temperature, under 30 MPa pressure and in vacuum – 10^{-3} Pa. Perlite from Aragats contains 96 mas % of volcanic glass. The phase composition of the obtained composite provides high physical and technical properties of these nanocomposites: compression strength-2198 MPa, bending strength-271 MPa, coefficient of thermal expansion a20-700-3.8 10^{-6} °C. © *2024 Bull. Georg. Natl. Acad. Sci.*

nanocomposite, hot press, electron microscope, phase composition, B_4C-BN-TiC-TiB_2-SiC-β-SiALON-Al_2O_3 system

Composites working at high temperatures should be characterized by high density, hardness, thermal resistance and the ability to retain these properties at high temperatures. Composites obtained from highly refractory oxide ceramics maintain their hardness at high temperatures but they are characterized by a high coefficient of thermal expansion and therefore, low thermal resistance. Carbide-based ceramics have a relatively high coefficient of thermal expansion, but tend to oxidize easily at high temperatures. To address these challenges, the focus of scientific research has shifted towards developing super high-strength composites – SiALONs [1-4]. The results of our work indicate that the composites obtained with the SiALON matrix are highly refractory materials with high performance properties which they retain at high temperatures. For our study, we used electron microscopy, optical and X-ray phase analysis methods [5].

The paper describes the preparation of a super-ceramic composite with high macro and micro-mechanical properties of SiALON carbide at relatively low temperatures using an innovative, simple technology. As is known, SiALONs are obtained at temperatures of 1800-2000°C. However, by using vitrified perlite (96 mas. % glass phase) with 2-3 mas.% dopant, we obtained similar material at 1450°C. Furthermore, in combination with titanium carbide, boron nitride, boron carbide, silicon carbide and aluminum oxide (nanopowder), we were able to obtain eutectic precipitation at relatively low temperature 1620°C through hot pressing. The material is extremely hard, causing damage to the diamond beads during treatment and a 3000 atmosphere water jet failed to cut the specimen.

The X-ray analysis was performed using the DRON-3 apparatus. Electron microscopic research was performed on a raster electron microscope „Nanolab 7" of the company „OPTON". No special form of samples is required for this study, only a sample fracture is needed.

To obtain the composites, we prepared mixtures, the composition of which is given in Table 1. To C-18 composite we have added carbon fiber, which is characterized by high elasticity modulus (200-935 GPa), high- tensile strength (1-3 GPa), with these properties it is the desired component, since it strengthens the composite material [6].

Table 1. Material composition of composites

Composition of the initial component, mass%												
Composite index	Kaolin (Ukraine)	TiC	Al	Al_2O_3	SiC	Si	Perlite Aragats (Armenia)	BN	Y_2O_3	MgO	B_4C	Carbon fiber
C-19	5	-	17	22	21	20	2	-	1.5	1	10.5	_
C-18	_	-	18	20	23	19	_	-	1.5	1	14.5	3
C-16	-	5	16	18	20	17	2	9	1.5	1	10.5	-
C-17	-	6	16	18	22	17	2	11	1.5	1	5.5	-

The samples were made in a cylindrical shapes using the semi-dry method, with a molding pressure of 20 MPa. After drying the samples were burned out in a silite oven at a temperature of 1450°C. Mode 5°C/min. Once reaching the final temperature the samples were kept for 40 minutes.

The bending strength was measured on a German-made disruption machine R-100, equipped with a device specifically designed to determine the strength limit of specimens under three-point bending conditions.

The test results of C-19 and C-18 composites are given in Table 2.

The impact viscosity was determined using the pendulum impact testing machine, where the swing angle of the pendulum, marked on a scale as β, indicates sample crush.

Impact-bending strength is derived from the formula:the sample is crushed, the scale marks the swing angle of the pendulum β. Impact-bending strength is derived from the following formula: $A_{imp.}$ =A/S where: A denotes work spent to crush sample, kilo Joules (kJ); S – the cross-sectional area of the samples, m^2. For the C-19 composite samples: the cross-sectional dimensions were 1 cm x 0.35 cm; $a = \frac{6,17}{1 \times 0,35}$ =17,62 kJ/m^2 ; for the C-18 composite samples: the cross-sectional dimensions were 1 cm x 0.2 cm; $a = \frac{6,17}{1 \times 0,34}$= 18.14 kJ/$m^2$. As can be seen from Table 2, the bending strength and the impact viscosity of both composites (C-19, C-18) are almost the same and amount to 262; 264 MPa and 17.62; 18.14 kJ/m^2

respectively. Ceramic composites experience thermal load sand gas-thermal impacts when working at high temperatures [7]. To determine these energies, Z. Kovziridze proposed a formula for calculating the failure stress energy, which establishes a universal interdependence between the failure stress energy of a product, the mass of the product, and the rate of crack development under critical stress conditions [8]. Z. Kovziridze's formula for calculating the failure stress energy is as follows: $E_{td} = ma_{c.p.}$, where E_{td} is the failure stress energy, kilo joules; m – sample mass, g; $a_{c.p.}$ – the crack development rate – 2000 m/sc. In our case the sample dimensions were 5.2 x 5.2 x 45 mm, the sample mass was 3.86 g. According to Z. Kovziridze's formula the failure stress energy is $E_{td} = ma_{c.p.} = 3.86 \times 2000 = 7.72$ kJ.

Table 2. The physical and technical characteristics of composites

Composite name	Density g/cm^3	Compression strength $\sigma_{press.}$MPa	Bending strength $\sigma_{bend.}$MPa	Impact viscosity a, kJ/m^2	Thermal expansion coefficient α, 10^{-6} (20-700°C)
C-19	3.11	1844.4	262	17.62	3.81
C-18	2.99	2189.8	264	18.14	3.83
C-16	3.12	2194.4	268	18.90	3.78
C-17	3.16	2198.5	271	18.80	3.82

The thermal expansion coefficient of the composites (C-19, C-18) was determined with the help of a quartz vertical dilatometer -DKV for measuring the temperature coefficient of linear thermal expansion in the temperature range (20-700°C). Table 2 shows that this indicator is the same for composites and is a = 3.88 and 3.80 • 10^{-6}, respectively.

Electrical characteristics have been established for the composite of compositions (on the device created by Prof. T. Cheishvili-CH-24) which were obtained as a result of the „resistance-temperature" dependence experiment. The volumetric electrical resistance of the composites was determined in the section allowing measurements at high-temperatures in the range of 20-300^{0}C, by using an electron ohm meter as the measuring instrument. Graphite electrodes were placed on the surface of the prismatic samples (the upper measuring electrode had a diameter of 14 mm and the lower measuring electrode had a diameter of 16 mm). The dependence of the test specimens on the "specific resistance-temperature" is linear, revealing the peculiarities that an increase in temperature causes a decrease in electrical resistance. Besides the C-19 specimen is characterized by lower values of electric resistance than the specimen C-18, C-16, C17. The difference between the electrical resistances is particularly noticeable at room temperature (the difference is approximately by three degree), but it is less evident at high temperatures (the difference decreases to one degree), which is clear from the material reflecting the results of the experiment (Fig. 1).

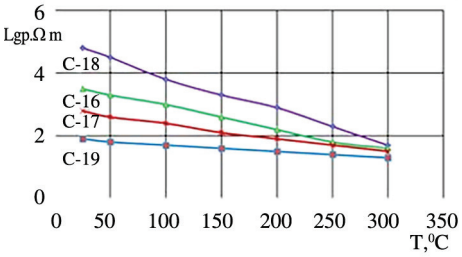

Fig. 1. Specific electrical resistance and temperature dependence.

Table 3. Electrical characteristics values of composites

Sample №	Coefficient of electrical sensitivity, B(ΩmK)	Activation energy of electrical conductivity, ΔE(ev)	Temperature coefficient of electrical resistance, $a\Delta_t$(ΩmK^{-1})
C-18	-7170	1.24	$-2.6.10^{-2}$
C-19	-1560	0.27	$-5.7.10^{-3}$
C-16	-1625	0.65	$-1.4.10^{-2}$
C-17	-815	0.32	$-6.8.10^{-3}$

The values of the electrical parameters of the investigated composites were calculated on the basis of the obtained "lgp- t" dependence. Three electrical characteristics were determined for composites: the temperature coefficients of electrical sensitivity (B) and electrical resistivity (α_T), along with the activation energy of electrical conductivity (Ea), the value of which are presented in Table 3. Notably, the composites exhibit a negative α_T (resistance decreases with increasing temperature) and low value of Ea- (realization of electronic type of electrical conductivity is expected for both materials).

The obtained results should be related to the basic phases represented in the C-19 and C-18 composites synthesized at 1450^0C, under the same conditions. Regarding the compositions C-16 and C-17, which exhibit "$\log_{p\text{-}T}$" dependences occupying an intermediate position between C-19 and C-18, it can be noted that the compositions contain two "new" ingredients – TiC and BN. In some high-temperature synthesis of composites, one cannot exclude the participation of these ingredients in the formation of a new semiconductor phase – TiB_2. Based on the compositions of C-16 and C-17, the expected amount of TiB_2 should be greater in C-17. This is also confirmed by the electrical properties in comparison with composition C-16; composition C-17 has lower values of resistivity and activation energy.

According to the results of the X-ray phase analysis, the leading phase in the composite of both compositions is SiALON. They also contain five other crystalline compounds of different nature. Due to their electrical properties they can be divided into two groups: dielectrics (a- Al_2O_3, BN, AlN) and semiconductors (SiC, Si). Considering the identical conditions for obtaining the C-19 and C-18 composites, the factor determining their low resistance and activation energy values could have been the number of SiC and Si solid phases with semiconductor properties existed in the study materials.

Based on the comparison of the electrical characteristics of composites, it can be assumed that the concentrations of SiC and Si in the C-19 composite must be higher than in the C-18 composite. This could be detected by two approaches: by determining the amount of SiC and Si or by the density of the materials. Both approaches proved to be unusable for C-19 and C-18 composites, since quantitative calculations based on the available X-ray were impossible (due to the abundance of crystal phases and the coincidence of their characteristic intensity peaks) and also the negligible differences between mass densities (d = 3.11 for C-19; d = 2.99 g/cm^3 for C-18). In any case, the number of SiC in C-19 could not have been higher than in C-18, judging by the material composition of the test composites.

At the same time, X-ray phase analysis revealed the presence of Si in both composites, which could affect the electrical conductivity of the composite. But the Si content in the initial mixture (according to the material compositions) is identical and amounts to wt. 20%. At the same time, the C-19 composite body contains two natural rocks (kaolin and perlite) that contain silicon dioxide. Kaolin (5 wt.%) and perlite (2.0 wt.%) provide approximately 5.2 wt.% and 3.0 wt.% Si in the C-19 composition, respectively. The reason for this is the structural breakdown of the mineral kaolinite in the geopolymer (kaolin) caused by

the temperature and the possibility of conducting the parallel alumothermic process: $4Al + 3SiO_2 = 2Al_2O_3 + 3Si$.

This process will result in an additional 2.4% by weight of Si in the C-19 composite, and it is practically expected that the amount of Si in C-19 will be 24.4% by weight. A contributing factor to the uptake of Si from SIO_2 may be the formation of a liquid phase caused by the low-temperature melting of perlite-1240^0C. Aluminum nitride is formed by the reaction of a portion of the aluminum powder in the initial mixture with nitrogen by the following reaction: $2Al + N_2 = 2AlN$.

Structural Study

The test specimens were prepared using the same technology as described in previous publications, i.e., the SiALON was synthesized in the nitrogen medium at 1400–1450^0C, and then the obtained mass was grounded in an attritor and the consolidated composite was obtained by hot pressing at 1620^0C, 40 minutes, delaying at final temperature for 8 min, under 30 MPa pressure [9-12].

70 μM of study samples of the composite obtained in this mode were cut from 70 mm diameter and 8 mm thick discs. The cut was made on a 395-M profile grinding machine with a 100 mm-diameter metal binding diamond cutting disc, diamond grain size 50/40 μm, cutter rotation speed 4000 rpm, cutting speed 0.7 mm/min.

The surface of the cut specimens was ground on a 3G71 flat-bottomed grinding machine with a 200 mm- diameter diamond abrasive disc on a Bakelite binder, diamond grain size-50/40μm.

Phase analysis of hot-pressed samples was performed on the X-ray machine DRON-3 using CuKα rays.

Examination of the X-ray patterns of the samples burned out at 1400-1450^0C shows that at 1400^0C the characteristic reflexes of the SiALON are already observed in both composites, and at 1450^0C their intensity is relatively increased. Judging by the intensity of the characteristic peaks of the SiALON, the number of SiALONs formed in C-19 composite is relatively larger than in C-18 composite, which can be explained by the presence of kaolin in the C-19 composition. In our opinion, this is due to the nitrogenation of the thermodynamically active kaolinite core $Al_2O_3{\cdot}2SiO_2$, which was formed as a result of the decomposition of the mineral kaolinite. The following phases have been observed in both composites: Si-AL-O-N, SiC, α-Al_2O_3, BN, and Si (small amount unreacted.).

Part of boron carbide and titanium carbide in the composites was converted to boron nitride and titanium diboride upon burning out in nitrogen medium at 1400^0C by the following reaction: $B_4C+2N_2=4BN+C$, and $B_4C + 2TiC = 2TiB_2 + 3C$, which in the case of both composites is in small quantities. The newly formed, fine-grained boron nitride improves the microstructure, which is a prerequisite for achieving high mechanical properties, such as high thermal conductivity, low thermal expansion, good resistance to thermal shocks, easy workability, chemical inertness and low wettability with molten metals. It is used in radiators, boron-alloyed silicon semiconductors, welding trays, crucibles, microwave tubes, sputtering targets, high-precision welding, foundry production, etc.

The analysis performed using an optical microscope showed that the composites consisted of silicon carbide and corundum grains located in the matrix. At the same time, the microstructure of C-18 composite is more fine-grained. It can be assumed that during the sintering process of the C-19 composite, due to its composition, more liquid phase is generated than during the sintering process of C-18, contributing to the sintering intensity, which is evidenced by the relatively low porosity of C-19 composite. At the same time,

the liquid phase promotes the appearance of small grains and their subsequent recrystallization into large grains.

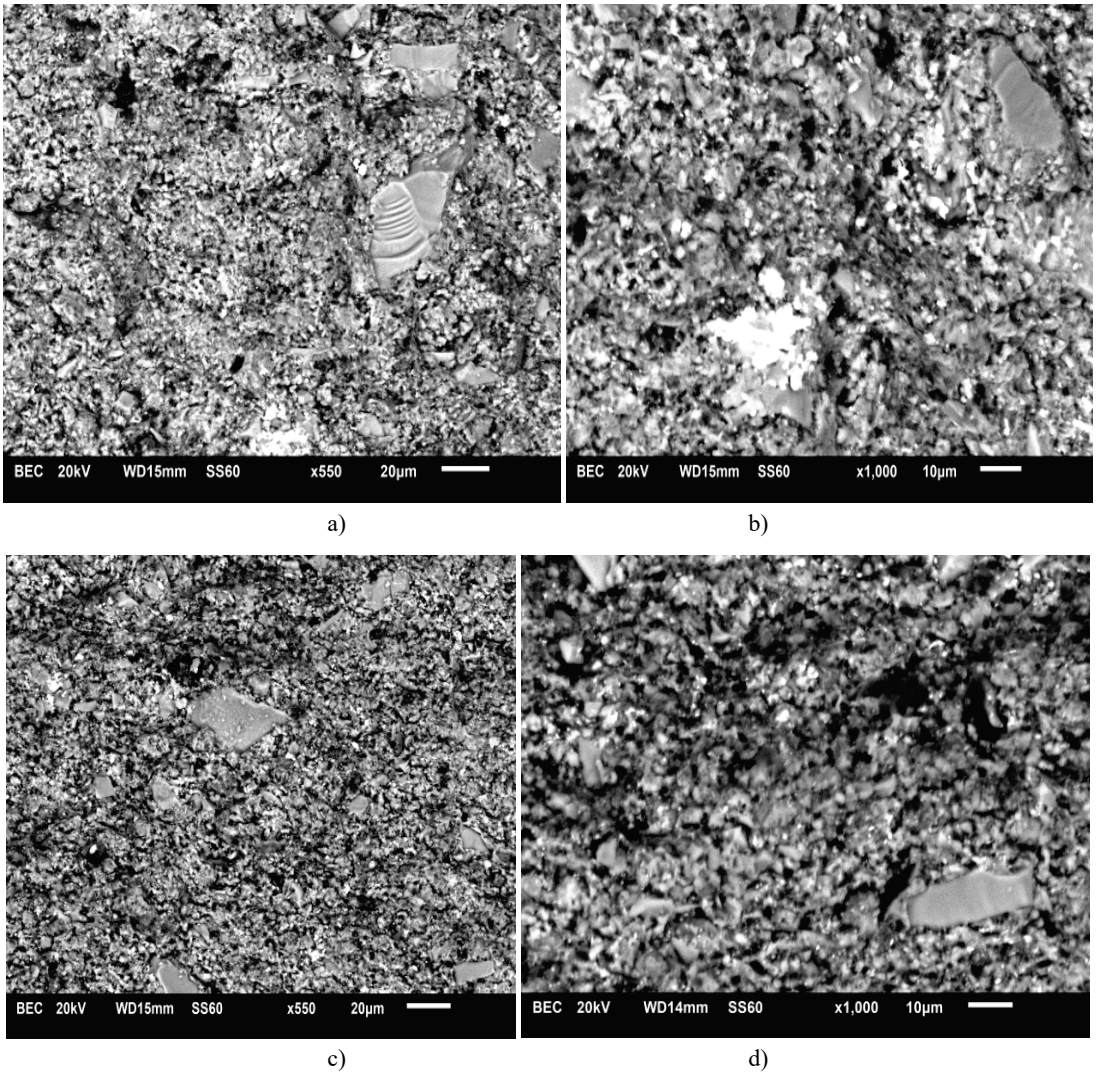

Fig. 2. C -19 (a, b) and C -18 (c, d) composites. Electron microscopic images at different magnifications.

Electron microscopy shows the surface of a well-sintered specimen, revealing crystals of the basic phases contained in C-19 composites, namely silicon carbide and corundum grains distributed in the SiALON matrix. Even the finest grains of boron nitride are also observed, which are better seen when magnified at close-up (Fig. 2). The results of electron microscopy of the given composites are consistent with X-ray structural analysis. In the matrix of composites C-19 and C-18, there are represented: β-SiALON-Al_2O_3-SiC, BN crystals are distributed in the matrix. In the composites CH-16 and CH-17, there are represented TiC-TiB_2-BN-SiC-B_4C-β-SiAlON-Al_2O_3 phases. Table 4 shows the data on phase components in C-19 and C-18 composites.

To determine the porosity, we selected the field of vision and determined its area. In the field of vision, we calculated the number of pores according to the size of their diameter; determined the volumetric content and the middle diameter of pores for each composite. The total pore content in C-19 composite is

approximately P_{vol} = 3,7%, for C-18 -Pvol = 4,8%, the middle size of the pores makes up $P_m \approx 3{,}75$ and 4.5 μM, respectively.

Table 4. The data on phase components in C-19 and C-18 composites

Composite	Phase name	Field of vision S, μM²	Number of counted grains (pores), n	Grains (pores) Dmid. μM	Max. size of grain (pore) Dmax. μM (average)	Min. size of grain (pore) Dmin. μM (average)	F_{Kf}–shape factor Dmax/Dmin
C-19	SiC	2070	12	11	9	3	
	Al_2O_3		250	1	1	1	
	SiALON BN		55 45	14 0.2	32 0.25	18 0.16	
	Average		90.5	6.5	10.56	5.54	1.91
	Pores		10	3.75	4	3.5	1.15
C-18	SiC	2070	15	10	8	4	
	Al_2O_3		280	0.8	1	0.8	
	SiALON BN		50 45	9 0.22	33 0.27	20 0.18	
	Average		97.5	6.6	10.56	6.25	1.69
	Pores		12	4.5	5	4	1.25

In the C-19 composite, the maximum and minimum sizes of SiC grains is 9-3 μM, middle size = 6 μM; in C -18 composite - 8-4 μM, middle size = 6 μM.

The maximum and minimum size of aluminum oxide grains is 1 / 1μM for C-19 composite and 1/0.8 μM for C-18 composite. The average size of aluminum oxide grains in each composite ranges from 1 to 0.8 μM, respectively. As for boron nitride, its dimensions are minimal and approximately equal to an average of 200 nM. The total average grain size is Km = 6.5 and 6.6 μM, respectively. The glassy phase volume fraction Gvol = 3 and 1%, respectively, with crystal shape factor being:

$F_{kf}c_{-9}$=Dmax/Dmin=10.56/5.54=1.91;

$F_{kf}c_{-10}$=Dmax/Dmin=10.56/6.25=1.69.

Crystal distribution factor in the matrix by our visual estimation, F_{kd} = 0.9.

The unreacted residue of silicon is about 2 wt.%. In instances where the silicon mass exceeds the initial composition, it should not surpass 18-19 percent. The carbon fiber dopant increased the mechanical properties by 3 wt.% in C-18 (Table 2). The crystalline phase content is calculated as follows: in C-19, 100-(V porous +V glassy)=100-(3.7+3) =93.3, while in C-18: 100-(V porous++V glassy) = 100-(4.8 + 1) = 94.2.

The dependence of the micro- and macro- mechanical characteristics of the materials on the crystalline phase content in the composite was calculated according to Z.Kovziridze's formula [13].

$$\sigma_d = \frac{\text{P.Fkd}}{\text{Km Kv Fkf}},$$

where: P denotes the load; K_m – the average size of the crystals; K_v- the volume fraction of crystals in the matrix; F_{kd} is the crystal distribution factor in the matrix, determined by the researcher. In the case of equal distribution, it equals 1; in the case of unequal distribution, it equals 0.9; F_{kf} is crystal shape factor, taken as the ratio of the largest characteristic size of a crystal to the smallest. This factor allows us to characterize the shape of a given set of crystals, according to which we are able to define correlation of mechanical characteristic in the matrix from the crystal phase characteristics in our proposed formula. By inserting the data from Table 4 into the formula, we get: $\sigma_d = \frac{2187.5 \text{ x } 0.9}{6.5 \text{ x } 94.2 \text{ x } 1.69} = \frac{1968.75}{1035} = 1.9$.

The dependence of the macro-mechanical characteristics of the materials on the porous phase content in the composite was also determined according to Kovziridze's formula [15].

$$\sigma_{m/p} = \frac{P}{F_p \cdot P_d \cdot P_{vol} \cdot P_m} = \frac{2187.5}{0.9 \text{ x } 1.25 \text{ x } 4.5 \text{ x } 4.8} = \frac{2187.5}{24.3} = 90 \text{ MPa}/\mu M^2 ,$$

where P is the load in MPa; F_p – the shape factor of the pores; P_d - the pores distribution factor in the matrix. Determination of this value and the evaluation of its significance depends on the researcher, based on the morphological picture depending on how the pores are distributed in the material and their size. The value of the factor can vary from 1 to 0.8. If the pores are evenly distributed in the matrix and are about the same size, the factor is determined to be equal to 1. If the pores are unevenly distributed, the factor equals to 0.9 and if the coalescence process of pores is initiated, factor is 0.8; P_{vol} – volumetric fraction of the porous phase in the matrix; P_m – the average size of the pores.

Conclusion

The phase composition of the obtained composites was studied, revealing a main matrix phase of TiC-TiB_2-B_4C- SiAlON-SiC-BN-Al_2O_3, in which the BN grains are distributed, originated in the nitrogenation process as a result of the decomposition of boron carbide by nitrogen and substitution of carbon with nitrogen. The composites exhibit robust sintering, with crystals bonded together by a SiAlON layer, resulting in materials with high physical and technical characteristics.

The advantage of this method is that compounds, which are newly formed thanks to interaction going on at thermal treatment: Si_3N_4, Si, AlN are active, which contributes to **β**-SiALON formation at relatively low temperature, at 1300-1350°C. It is evident that inculcation of ALN in crystal skeleton of ß-Si_3N_4 is easier since at this temperature interval crystal skeleton of Si_3N_4 is still in the process of formation. ß-SiAlON was formed at 1450°C. Part of the boron carbide was transformed into boron nitride and titanium diboride in a nitrogen-rich nitrogen environment, although in both composites these compounds are present in relatively small quantities. The composite exhibits low resistance (specific resistance approximately 10^2 Ohm·m), with an activation energy (E = 0.27 eV) and the temperature coefficient of electrical resistance (Δα T = 0.057 k^-1). It primarily consists of β-SiAlON. The material demonstrates a compression strength of 2198 MPa, bending strength of 271 MPa, and a Vickers hardness (HV) of 1368. The thermal expansion coefficient between 20°C and 700°C is -3.8 x 10^-6 °C.

We express our gratitude to Shota Rustaveli Georgian National Science Foundation of Georgia, FR-21-1413 Grant 2022.

მასალათმცოდნეობა

ჭკვიანი ნანოკომპოზიტი TiC-BN-SiC-B_4C-SiAlON-Al_2O_3 სისტემაში ტურბინების დისკებისა და ფრთებისთვის, ბალისტიკური ჯავშანტექნიკისთვის, საფრენი აპარატების ცხელ კვანძებში სამუშაოდ

ზ. კოვზირიძე*, ნ. ნიჟარაძე*, მ. მშვილდაძე*, გ. ტაბატაძე*, თ. ჭეიშვილი*, ც. დანელია*, ნ. დარახველიძე*, მ. ბალახაშვილი*, ს. გვაზავა*

* *საქართველოს ტექნიკური უნივერსიტეტი, ბიონანოკერამიკისა და ნანოკომპოზიტური ტექნოლოგიის ინსტიტუტი, ბიონანოკერამიკისა და ნანოკომპოზიტური მასალების სამეცნიერო ცენტრი, თბილისი, საქართველო*

(წარმოდგენილია აკადემიის წევრის ვ. ციციშვილის მიერ)

ჩვენი მიზანი იყო პირველ ეტაპზე β-SiALON შემცველი ნანოკომპოზიტების მიღება რეაქციული შეცხობის მეთოდით 1400°C ტემპერატურაზე, აზოტირების პროცესით TiC-BN-SiC-B_4C-Si-Al-Al_2O_3 (ნანოფხვნილი) სისტემაში. სინთეზის ამ მეთოდის გამოყენებით შესაძლებელი გახდა ნანოკომპოზიტების მიღება მატრიცაში β-SiALON-ის სხვადასხვა მასური პროცენტით. ჩვენი ამოცანა იყო TiC-TiB_2-BN-SiC-B_4C-β-SiAlON-Al_2O_3 სისტემაში მიღებული კონსოლიდირებული მასალების მიღება და ფაზური შედგენილობის შესწავლა. მიღებული მასა დაიფქვა ატრიტორში და კონსოლიდირებული კომპოზიტი მიიღება ცხელი წნეხვით 1620°C ტემპერატურაზე 40 წუთის განმავლობაში, მინისებური არაგაცის პერლიტის (სომხეთი) დოპირებით 2 მას.%, საბოლოო ტემპერატურაზე 8 წუთის დაყოვნებით, 30 მპა წნევის ქვეშ და ვაკუუმში – 10^{-3} Pa. პერლიტი არაგაციდან შეიცავს 96 მას. % ვულკანურ მინას. მიღებული კომპოზიტის ფაზური შედგენილობა უზრუნველყოფს ამ ნანოკომპოზიტების მაღალ ფიზიკურ-ტექნიკურ თვისებებს: მექანიკა კუმშვაზე-2198 მპა, სიმტკიცე ღუნვაზე-271 მპა, თერმული გაფართოების კოეფიციენტი $a_{20-700} = 3.8\ 10^{-6}$ °C.

REFERENCES

1. Osman S., OrhanU., Malgorzata S., Gocmez H., Kolemen U. (2008) Dynamic hardness and elastic modulus calculation of porous SiAlON ceramics using depth-sensing indentation technique. *Journal of the European Ceramic Society,* 28: 1235–1242.
2. Hou Z., Ye F., Liu L. (2015) Effects of pore shape and porosity on the dielectric constant of porous β-SiAlON ceramics. *J. Eur. Ceram. Soc.*, 35: 4115–4120.
3. Li B., Liu K., Zhang C.R., Wang S.Q. (2014) Fabrication and properties of borazine derived boron nitride bonded porous silicon aluminum oxynitride wave-transparent composite. *J. Eur. Ceram. Soc.,* **34** (15): 3591–3595.
4. Yang J.F., Beppu Y., Zhang G.J., Ohji T., Kanzaki S. (2002) Synthesis and properties of porous single-phase β-SiAlON ceramics. *J. Am. Ceram. Soc.*, **85** (7): 1879–1881.
5. Kovziridze Z., Nizharadze N., Tabatadze G., Cheishvili T., Mestvirishvili Z., Nikoleishvili E., Mshvildadze M., Darakhvelidze N. (2014) Obtaining of nanocomposites in SiC-SiAlON and Al_2O_3-SiAlON system by alumothermal processes. *Journal of Electronics Cooling and Thermal Control,* 4: 105-115. http://dx.doi.org/10.4236/jectc.2014.44012.
6. Kovziridze Z., Nizharadze N., Tabatadze G., Darakhvelidze N., Mestvirishvili Z. (2016) Smart materials in the system SiAlON-SiC- Al_2O_3-TiB_2-ZrB_2, Bit's 2nd Annual World Congress of Smart Materials, p. 558. Singapore.
7. Griffith A. (1921) Trans. Roy. Soc. A. 221, pp. 163-198. London.
8. Kovziridze Z. (2018) Failure stress energy formula. *Journal of Electronics Cooling and Thermal Control,* 8: 31-47. Http:www.scirp.org/journal/jectc.
9. Kovziridze Z., Nizharadze N., Tabatadze G., Cheishvili T., Darakhvelidze N., Mestvirishvili Z., Mshvildadze M., Nikoleishvili E. (2014) Obtaining SiAlON-s by nitroalumthermal processes, Georgian Ceramics Association, *Journal „Ceramics and Advanced Technologies",* **2** (32): 23-31.
10. Enquan H., Jianshe Y., Lei F., Chao W., Hongjie W. (2011) Synthesis of single phase b-SiAlON ceramics by reaction-bonded sintering using Si and Al_2O_3 as raw materials. doi:10.1016/j. scriptamat. 2011.03.040.
11. Peng J., Xiao fang W., Wendong X., Junhong Ch., Wei W., Yong L. (2015) In-situ synthesis and reaction mechanism of β-SiAlON in the Al-Si_3N_4-Al_2O_3 composite material https://www.researchgate.net/publication/282632023_In-situ_synthesis_mechanism_of_plate-shaped_b-Sialon_and_its_effect_on_Al_2O_3-C_refractory_properties.
12. Kovziridze Z. (2020) The formula of dependence of mechanical characteristics of materials on crystalline phase composition in the matrix. *Advances in Materials Physics and Chemistry,* **10**, 8, ISSN: 2331-1959. DOI: 10.4236/ampc.2020.108013 .
13. Kovziridze Z. (2018) Macro-mechanical properties porous phase dependence formula. Journal of the Georgian Ceramists Association. *Ceramics and Advanced Technologies.*, **20** 1(39): 28-34.

Received February, 2024